I&EC research
Industrial & Engineering Chemistry Research

pubs.acs.org/IECR

Article

Curing Kinetics of Main-Chain Benzoxazine Polymers Synthesized in Continuous Flow

Zhou Zhou, Qian Si, Li Wan, Shiao-Wei Kuo, Changlu Zhou,* and Zhong Xin*

Cite This: *Ind. Eng. Chem. Res.* 2022, 61, 2947−2954

Read Online

ACCESS | Metrics & More | Article Recommendations | Supporting Information

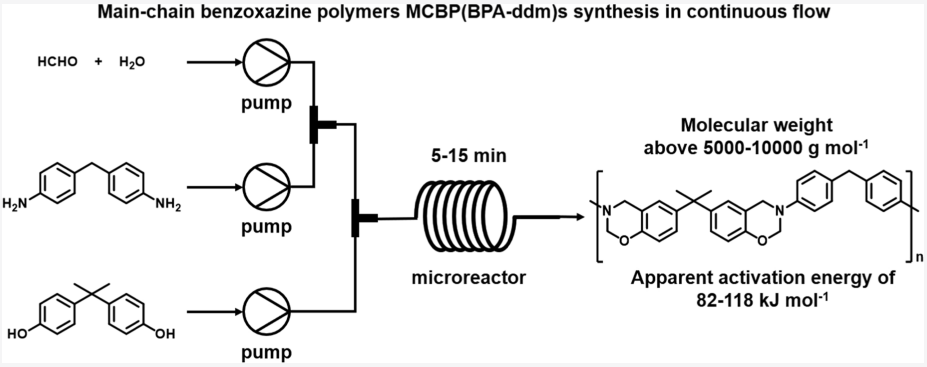

ABSTRACT: Main-chain benzoxazine polymers MCBP(BPA-ddm)s were synthesized in continuous flow under various residence times of 5, 10, and 15 min. MCBP(BPA-ddm)s with high molecular weight above 5000−10 000 g mol^{-1} and high purity over 93% oxazine ring-closed ratio were obtained, which were characterized using Fourier transform infrared (FTIR) spectroscopy, nuclear magnetic resonance spectroscopy, and size exclusion chromatography. *In situ* FTIR spectroscopy and differential scanning calorimetry were performed to understand the curing reaction and kinetics of MCBP(BPA-ddm)s, suggesting a typical thermally driven self-catalyzed ring-opening polymerization profile with an apparent activation energy of 82−118 kJ mol^{-1}, which follows first-order curing kinetics regardless of the molecular weight.

1. INTRODUCTION

Because of its high modulus and thermal stability, outstanding flame-retardant and dielectric abilities, and significant hydrophobic performance, polybenzoxazine (PBz) has found widespread applications in many fields, such as aerospace, transportation, the oil/gas industry, electronic manufacturing, and so on.[1−3] Typically, benzoxazine (Bz) monomers can be synthesized using any combination of a phenolic derivative, a primary amine, and formaldehyde as starting materials, which offers rich molecular design flexibility to the Bz family and allows for tailoring PBz's properties to meet the requirements for specific applications.[4−7] Especially, cross-linked PBz prepared from the main-chain Bz polymers (MCBPs) does not only exhibit excellent performance as classical systems of mono- or difunctional Bz but also shows enhanced ductile and thermal properties on increasing the molecular weight of monomers.[8−10] However, complex products' constitution is particularly problematic according to the mechanism of Bz synthesis, as shown in Figure 1, which is highly sensitive to the ratio of reactants. Therefore, a washing procedure with water, acid, or alkaline solution is an indispensable component of the typical process of Bz synthesis to eliminate byproducts and a waste of time and resources to some extent.[11−13] In the case of MCBP synthesis, this situation is a more significant challenge for the control of molecular weight distribution and reaction time.

The past several decades have witnessed various approaches for MCBP synthesis, which was reported firstly in 1995 by using 4, 4′-methylenebis(2,6-dimethylaniline), bisphenol A, and formaldehyde.[14] The method of diamines and bisphenol polycondensation to produce an AABB-type MCBP was further conducted by Takeichi et al. and Chernykh et al.[15,16] Extensive efforts have been made in the field of MCBP synthesis over the following years. In the classic AABB method, a linear MCBP with large oligomeric sizes (1000 < the number average molecular weight (M_n) < 10 000) is obtained by a single-step reaction between diamines, bisphenol, and formaldehyde with a molar ratio of 1:1:4. After polymerization, the resulting PBzs from MCBPs show increased tensile strength and elongation at break due to the linear structure of MCBPs

Received: December 5, 2021
Revised: February 1, 2022
Accepted: February 3, 2022
Published: February 15, 2022

https://doi.org/10.1021/acs.iecr.1c04771
Ind. Eng. Chem. Res. 2022, 61, 2947−2954

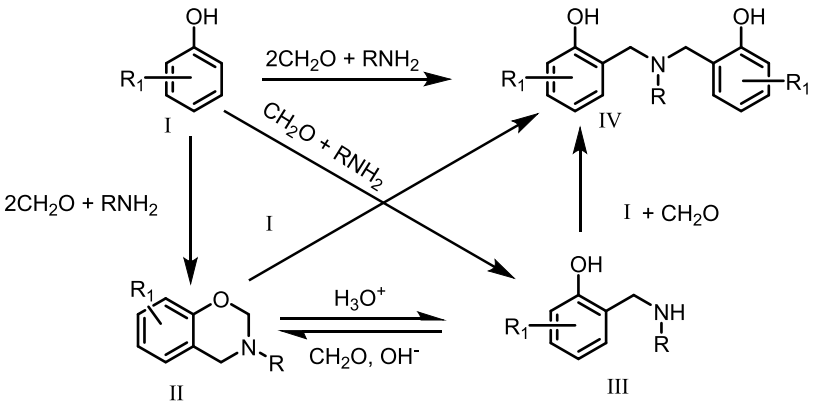

Figure 1. Mechanism of benzoxazine synthesis proposed by Burke: I, phenolic compound; II, benzoxazine; III, Mannich base, and IV, dimer with a Mannich bridge.

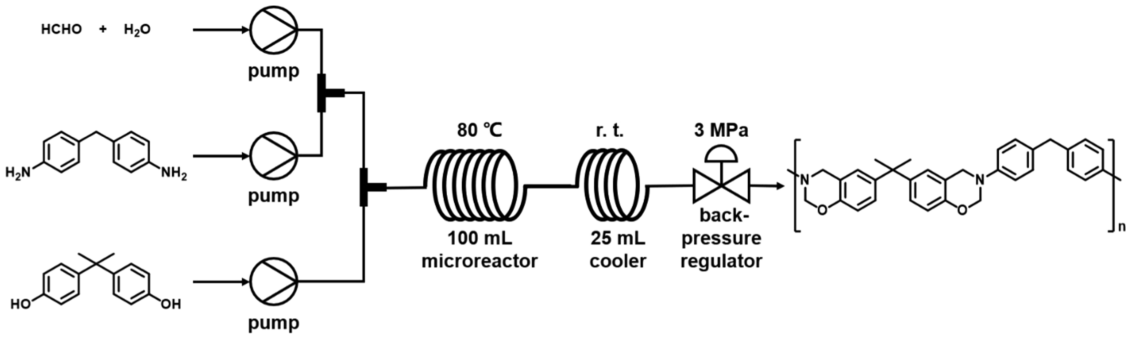

Figure 2. Synthesis route of MCBP(BPA-ddm) by continuous flow.

with higher molecular weight.[15−17] In this way, some amine-terminated compounds such as siloxanes or polyether could be used instead of diamines in the AABB approach. Improvement in thermal stability or processing ability was verified due to the incorporation of polydimethylsiloxane or Jeffamines, respectively.[18−20] Besides the AABB-type MCBP, Agag and Takeichi carried out the self-condensation of aminophenols and related derivatives in the presence of formaldehyde to form AB-type MCBPs. The char yield of cross-linked AB-type MCBPs was reported to be as high as 67%.[21] However, it is difficult for polycondensation via the Mannich reaction approach to maintain the stoichiometry during the condensation reaction due to many side reactions, resulting in MCBPs with low molecular weight.[14] Although novel Bz monomers with many reactive end groups (e.g., ethynyl, propargyl, allyl, alcohol, and so on) have been designed to overcome these difficulties to some extent, the versatility and molecular flexibility of MCBPs are limited severely by these approaches.[22−26]

In recent years, continuous-flow reactors with channel dimensions in the micro- or millimeter region have drawn increasing attention in organic synthesis owing to exceptional advantages such as large surface-to-volume ratio, high mixing efficiency, enhanced heat and mass transfer, excellent process safety, and so on.[27−29] Unlike synthesis in batch, the microstructured devices in continuous flow can easily achieve precise control of the reactant ratio over the whole process and virtually instantaneous mixing, avoiding time consumption on mass transfer and improving the reaction efficiency significantly. Similarly, the accumulation of heat and formation of hot spots can also be prevented in microscale reactors, which can reduce side reactions and improve the purity of products.[30,31] Only a few studies on Bz synthesized by the continuous method can be found in the database. Ishida et al. proposed an insightful idea for synthesizing Bz monomers without a solvent using continuous processing machinery which was by connecting a single-screw extruder to a Brabender Plasticorder to achieve this object.[32] Frazee presented the first relevant results concerning the potentialities of this continuous processing for Bz synthesis using a novel continuous high-shear reactor.[33] Therefore, the continuous flow technique provides great potential for process intensification of the Mannich reaction to overcome challenges for MCBP synthesis.

In this work, MCBP(BPA-ddm)s were synthesized from bisphenol A, 4,4-diaminodiphenyl methane, and formaldehyde in continuous flow. The structure, molecular weight, and molecular weight distribution of MCBP(BPA-ddm)s under various residence times were analyzed using Fourier transform infrared (FTIR) spectroscopy, nuclear magnetic resonance (NMR) spectroscopy, and size exclusion chromatography (SEC). *In situ* FTIR spectroscopy and differential scanning calorimetry (DSC) were carried out to understand the curing reaction and kinetics of MCBP(BPA-ddm)s. The apparent activation energy (E_a) and the curing reaction order (n) can be calculated using Kissinger and Crane methods.

2. EXPERIMENTAL SECTION

2.1. Materials. 2,2-Bis(4-hydroxyphenyl)propane (BPA, >98%) and 4,4-diaminodiphenyl methane (DDM, >98%) were purchased from Adamas Reagent, Ltd. Formaldehyde solution (37−40%) was purchased from Shanghai Sinopharm Chemical Reagent Co. Ltd. Toluene (≥99.5%), ethanol (≥99.7%), sodium sulfate (≥99%), and other chemicals were purchased from Shanghai Titan Scientific Co., Ltd. All of these reagents were used without further purification in all experiments.

https://doi.org/10.1021/acs.iecr.1c04771
Ind. Eng. Chem. Res. 2022, 61, 2947−2954

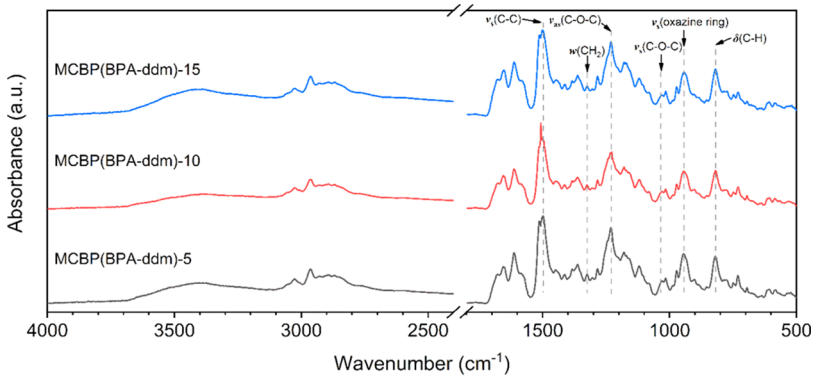

Figure 3. FTIR spectra of the MCBP(BPA-ddm)s obtained at various residence times.

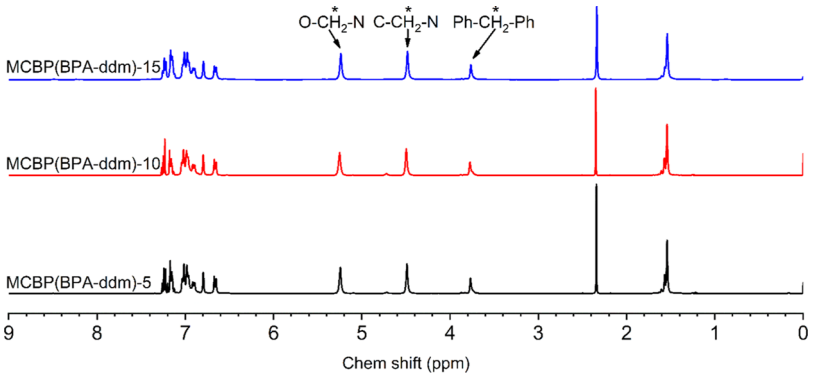

Figure 4. ^{1}H NMR spectra of MCBP(BPA-ddm)s obtained at various residence times.

2.2. Synthesis of Main-Chain Benzoxazine Polymer MCBP(BPA-ddm)s Using Continuous Flow. BPA (40 mmol) was dissolved in toluene (40 mL) and ethanol (15 mL). DDM (40 mmol) was dissolved in toluene (60 mL) and ethanol (35 mL). Formaldehyde (180 mmol) was obtained from a commercial formaldehyde solution. The structure of the continuous-flow reactor is displayed in Figure 2. Three plunger pumps were utilized to deliver the BPA, DDM, and formaldehyde solution into the microreactor, which is a coiled stainless steel tube with a diameter of 1 mm and a volume of 100 mL at a temperature of 80 °C. After the microreactor, a coiled stainless steel tube (1 mm i.d.) with a volume of 25 mL was used in the flow to cool the reaction mixture, which is performed at room temperature. A back-pressure regulator with 3 MPa was attached at the end of the system to avoid any gasification during the reaction. The residence time of the reaction was controlled by adjusting the liquid flow rate. The exiting reaction mixture in the first reaction period was discarded to ensure steady-state data collection. Then, 120 mL of the reaction mixture was collected, diluted with dichloromethane, and washed with deionized water subsequently. The organic phase was separated and distilled out to obtain a yellow solid, which is MCBP(BPA-ddm).

2.3. Characterization. Fourier transform infrared (FTIR) spectroscopy was performed on a Nicolet iS10 FTIR spectrometer (USA) with 32 scans at a resolution of 4 cm^{-1} using the KBr pellet method at room temperature (25 °C). Time-dependent FTIR spectra were recorded every 1 min with 16 scans at a resolution of 4 cm^{-1} from 50 to 300 °C at a heating rate of 10 °C min^{-1}. ^{1}H nuclear magnetic resonance (NMR) spectra were measured on Bruker Avance III 400 and Varian Mercury 400 spectrometers (Germany). Coupling constants (J) are given in Hz. Deuterated chloroform was used as a solvent for NMR measurement. Size exclusion chromatography (SEC) was carried out on a PL-GPC50 of Agilent Technologies, Inc. with UV or refractive index detection. A TA Q2000 differential scanning calorimeter (DSC, USA) was utilized at a constant flow rate of 50 mL min^{-1} under nitrogen at multiple heating rates of 2, 5, 10, 15, and 20 °C min^{-1} for the thermal curing analysis of MCBP(BPA-ddm)s.

3. RESULTS AND DISCUSSION

3.1. MCBP(BPA-ddm) Synthesis Using Continuous Flow. MCBP(BPA-ddm)s were synthesized after 5, 10, and 15 min of reaction in continuous flow, which are labeled as MCBP(BPA-ddm)-5, MCBP(BPA-ddm)-10, and MCBP-(BPA-ddm)-15, respectively. The structures of MCBPs were characterized using FTIR and NMR spectroscopies. IR spectra of the MCBP(BPA-ddm)s are shown in Figure 3. It features an obvious absorption band of benzoxazine functionality at 942−943 cm^{-1} (stretching vibration of oxazine ring), 1029 and 1230 cm^{-1} (symmetric and asymmetric stretching vibration of C−O−C in the oxazine ring, respectively), and 1325 cm^{-1} (CH_2 wagging of oxazine ring).[8,34−36] Additionally, a band at 818 cm^{-1} is observed, which is attributed to the out-of-plane bending of C−H in the 1,2,4-trisubstituted benzene ring. This is also supported by the characteristic band assigned to the in-plane symmetric stretching of C−C in the 1,2,4-trisubstituted benzene ring at 1498 cm^{-1}, which appears as a doublet with a similar band in the 1,4-disubstituted benzene ring of the DDM unit in the MCBP backbone.[8,37] The broad absorption band at around 3400 cm^{-1} identifies the terminated aminomethylol and OH groups of MCBP(BPA-ddm).[15,16,38]

https://doi.org/10.1021/acs.iecr.1c04771
Ind. Eng. Chem. Res. 2022, 61, 2947−2954

Figure 4 shows the ^{1}H NMR spectra of MCBP(BPA-ddm)s. The structure of benzoxazines is confirmed by the well-distinguished resonances of the methylene protons O−CH_2−N and O−CH_2−N of oxazine at 5.24 and 4.48 ppm, respectively. Additionally, the chemical shift at 3.77 ppm is attributed to the methylene protons Ph-CH_2-Ph of DDM. Although the terminated aminomethylol or OH groups are detected using FTIR spectra in Figure 3, no obvious signal of phenolic OH at 8−9 ppm in Figure 4 shows slight ring-opening of oxazine linkage or other side reactions in the continuous-flow reactor.[9] More specifically, the ratio of the chemical shift at 5.24 and 3.77 ppm is calculated to achieve a better understanding of the ratio between the ring-closed and ring-opened structures of oxazine in MCBP(BPA-ddm)s, which is 94:6, 93:7, and 94:6 for MCBP(BPA-ddm)-5, MCBP(BPA-ddm)-10, and MCBP(BPA-ddm)-15, respectively, suggesting their high purity in this work. However, a triazine signal at 4.72 ppm is detected for the sample with a residence time of 5 min, which decreases gradually with an increasing residence time till it disappears after 15 min of reaction. It is evident that the reactants can only react completely without triazine intermediates as byproducts after sufficient time, which is 15 min in this system. Both FTIR and ^{1}H NMR results confirm the structure of MCBP.

The average molecular weight of MCBP(BPA-ddm)s was characterized using SEC, and the results are listed in Table 1.

Table 1. Molecular Weight of MCBP(BPA-ddm)s

residence time (min)	M_n	M_w	M_z	M_v	PD
5	3093	10 339	27 868	8629	3.34
10	2594	7964	21 021	6796	3.07
15	1824	5273	12 881	4540	2.86

Generally, it usually takes 30−45 min to achieve an optimum reaction at 80 °C for traditional mono- or difunctional benzoxazine monomer synthesis by the static solventless method.[32] More specifically, more than 5 h of reaction time is required to obtain MCBP precursors with high molecular weight by the batch solution method.[8,9,39] In comparison, the time efficiency for MCBP synthesis is considerable by continuous flow. The number average molecular weight (M_n) and the weight average molecular weight (M_w) of MCBP(BPA-ddm) with the residence time of 5 min is 3.1×10^3 and 1.0×10^4 g mol^{-1}, respectively. However, the polydispersity (PD) of MCBP(BPA-ddm)-5 is high, and the M_n and M_w decrease on increasing the residence time. The possible reason for this tendency may be explained by the change of flow pattern in the microreactor, which can be predicted by the Reynolds number (*Re*, eq 1)

$$Re = \frac{\rho u d}{\mu} \tag{1}$$

where ρ is the density of the fluid (kg m^{-3}), u is the flow speed (m s^{-1}), d is the hydraulic diameter of the pipe (m), and μ is the dynamic viscosity of the fluid (Pa·s).

Flows in the microreactor tend to be dominated by laminar flow at low Reynolds numbers and turbulent at high Reynolds numbers. In our system, the diameter and length of the microreactor are fixed. Because of the low concentration (~0.2 mol L^{-1}) of reagents, the density and viscosity of the dilute reaction solution can be assumed to be constant during the reaction. Thus, *Re* number is proportional to the flow rate and inversely proportional to the residence time. According to eq 1, the flow in the microreactor tends to be turbulent with a well-mixed state along the radial direction at low residence time, which allows for the molecular chains not only to collide with each other but also to grow into big molecular chains with a high M_w. On the other hand, the linear molecular chains grow and become close to each other, and the molecular weight of all molecules tends to be similar in a long reaction time, which is why the PD decreases with an increasing residence time. Therefore, the MCBP with high molecular weight and low PD could be synthesized by continuous flow with a high flow rate and long residence time. The studies on such potentials are currently underway in our laboratory.

3.2. Curing Reaction Profile of MCBP(BPA-ddm)s. It is well established that the polymerization of benzoxazines is a thermally driven self-catalyzed cationic ring-opening process (ROP).[40,41] The high content of residual phenolic −OH groups in the monomer with a high ring-opened ratio initiates the ROP easily. After being triggered by the residues, the phenolic −OH groups generated from the benzoxazine catalyze and promote the curing reaction to form the polymer. The polymerization behavior of MCBP(BPA-ddm)s was monitored using *in situ* FTIR analysis, as shown in Figures 5 and S1, to gain a better understanding of the curing reaction. The characteristic absorption bands of the oxazine ring, i.e., ν_s(oxazine), ν_s(C−O−C), ν_{as}(C−O−C), and w(CH_2), gradually decrease as a function of temperature and completely disappear at 260°C, suggesting that the ROP proceeds. Meanwhile, constitution alternation of −OH multiple broad-

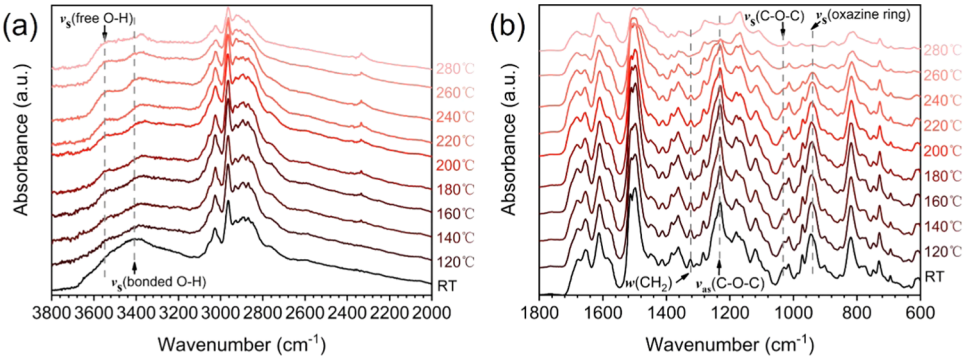

Figure 5. *In situ* FTIR spectra of MCBP(BPA-ddm)-5 from RT to 280°C over the regions of 3800−2000 cm^{-1} (a) and 1800-600 cm^{-1} (b) and intensity corrected by the vibrational band (benzene) at 1613 cm^{-1}.

https://doi.org/10.1021/acs.iecr.1c04771
Ind. Eng. Chem. Res. 2022, 61, 2947−2954

bands is observed from 3200 to 3600 cm^{-1} due to the release of phenolic −OH groups by the ROP.

At RT, the absorption corresponding to the intermolecular hydrogen bond between terminated −OH groups of the MCBP(BPA-ddm)-5 monomer is detected at around 3400 cm^{-1}, and no obvious absorption associated with free −OH at around 3530 cm^{-1} is observed in Figure 5a.[42] Therefore, the self-catalyzed effect of −OH groups is restricted when they are bonded and is activated by transforming to free −OH groups as the temperature increases, resulting in a shoulder peak at around 3530 cm^{-1}. The reactivity of −OH is unblocked and more −OH groups are released by the ROP with increasing temperature. Similar trends are also observed for MCBP(BPA-ddm)-10 and MCBP(BPA-ddm)-15, as shown in Figure S1. However, the relative variation between free −OH and bonded −OH is not obvious due to the formation of a more stable intramolecular −OH···N hydrogen bond resulting from the opened oxazine ring.

It is generally believed that the content of the organic groups in a compound is in line with the characteristic absorbance intensities of the corresponding peaks.[43] The qualitative information of the oxazine ring during the curing process can be obtained from the stretching vibration of the oxazine ring at 943 cm^{-1} due to its significance without obvious overlapping by other peaks. The vibrational band of benzene at 1613 cm^{-1} is used as the internal standard. The conversion vs polymerization time obtained from FTIR spectroscopy can be described using eq 2

$$\alpha = \left[1 - \frac{A_t(\text{oxazine})/A_t(\text{benzene})}{A_0(\text{oxazine})/A_0(\text{benzene})}\right] \times 100\% \quad (2)$$

where α is the conversion of oxazine ring and A_t and A_0 are the integrated areas of absorbance band at a given polymerization time (t) and the initial time, respectively.

Figure 6 displays the conversions of oxazine ring for MCBP(BPA-ddm)s during the curing process. A typical thermally driven self-catalyzed S-shaped profile is observed in Figure 6. The conversion remains almost zero in the first 12.5 min because the temperature <150 °C cannot initiate the ROP. The induction stage starts once the phenolic groups are released as autocatalysts. The reaction is usually slow at the induction stage due to the low concentration of autocatalysts. Further, more phenolic groups are formed as autocatalysts and the reaction is progressively accelerated, resulting in a dramatic increase of the conversion to >90%. All features are similar, as shown in Figure 6, for all MCBP(BPA-ddm)s regardless of the molecular weight.

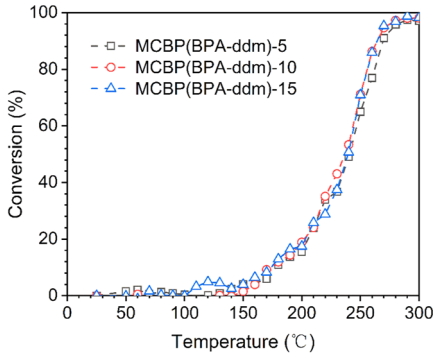

Figure 6. Conversions of the oxazine ring for MCBP(BPA-ddm)s during the curing process at a heating rate of 10 °C min^{-1} under an air atmosphere.

3.3. Curing Kinetics of MCBP(BPA-ddm)s. Differential scanning calorimetry (DSC) analysis thermograms in Figure 7 show the thermal curing information on MCBP(BPA-ddm)s at various heating rates. Table 2 shows the parameters of the nature of the curing reaction, such as initial curing temperature (T_i), peak temperature (T_p), and exothermic enthalpy (ΔH), at 10 °C min^{-1} from Figure 7a. One broad dominant exothermic peak of the curing reaction for all MCBP(BPA-ddm)s is observed at each reaction residence time or heating rate, implying the only one curing stage to form the cross-linking network for MCBP(BPA-ddm)s.[44,45] Two factors play a key role in the curing process of MCBP(BPA-ddm)s: the polymer chains with high molecular weight hinder their mobility to access each other and the sample with a high concentration of ring-opened structure cures more easily due to the catalytic effect of phenolic OH groups.[9,45] Taking the data on ring-closed and ring-opened structures in MCBP(BPA-ddm)s from NMR spectroscopy into account, MCBP(BPA-ddm)-5 with the highest molecular weight and ring-closed content exhibits the largest ΔH value of 214 J g^{-1}. As compared with MCBP(BPA-ddm)-5, less than 50% energy is required to cure MCBP(BPA-ddm)-10 and MCBP(BPA-ddm)-15. Although the molecular weight of MCBP(BPA-ddm)-10 is higher than that of MCBP(BPA-ddm)-15, the higher content of phenolic OH groups in MCBP(BPA-ddm)-10 makes its exothermic enthalpy lower than that of MCBP(BPA-ddm)-15.

As shown in Figure 7b−d, the nonisothermal DSC curves of MCBP(BPA-ddm)s at various heating rates were also detected to qualitatively evaluate their curing kinetics. As to MCBP-(BPA-ddm) synthesized at a certain residence time, its exothermic peak temperature shifts to a higher temperature on increasing the heating rate owing to the thermal hysteresis activity.[46] The apparent activation energy (E_a) and the curing reaction order (n) can be calculated using the Kissinger and Crane methods, which are believed to be sophisticated ways to deal with a complex thermoset curing process.[45,47,48] In the Kissinger method, E_a is calculated using the exothermic peak temperature without assuming any kinetic model and integration. Equation 3 is applied in the Kissinger method.

$$\ln \frac{\beta}{T_p^2} = \ln \frac{AR}{E_a} - \frac{E_a}{RT_p} \quad (3)$$

where E_a is the apparent activation energy of the curing reaction; T_p is the temperature of the exothermic peak, derived from the DSC curves in Figure 7b−d; and β, A, and R are the heating rate, Arrhenius constant, and universal gas constant (8.3145 J mol^{-1} K^{-1}), respectively.

In the Crane method, n is obtained using eq 4.

$$\frac{d \ln \beta}{d(1/T_p)} = -\left(\frac{E_a}{nR} + 2T_p\right) \quad (4)$$

where E_a is obtained by eq 3, n is calculated from the slope of $\ln \beta$ vs $1/T_p$ plot when E_a is much higher than $2T_p$.

The results of linear fitting using the Kissinger and Crane equations are presented in Figures 8 and S2. The relative coefficients (R^2) of MCBP(BPA-ddm)s approach 1, indicating a good linear relationship between the data and the model. The curing kinetic parameters are calculated and summarized in Table 2. The n and E_a values are 0.90−0.93 and 82−118 kJ

https://doi.org/10.1021/acs.iecr.1c04771
Ind. Eng. Chem. Res. 2022, 61, 2947−2954

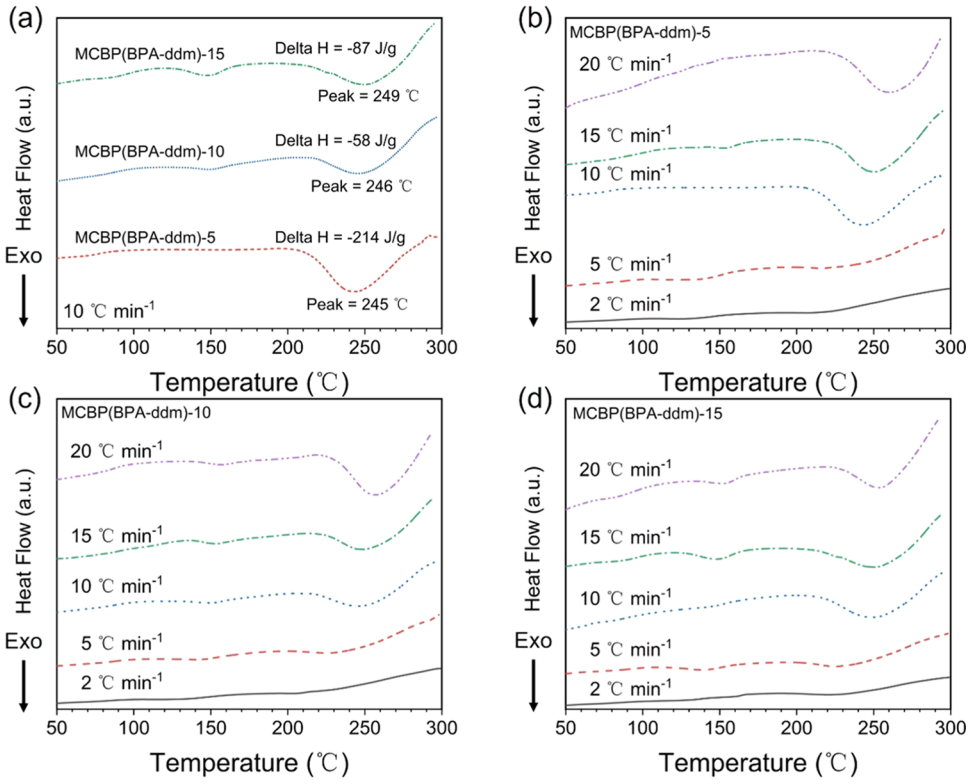

Figure 7. (a–d) Nonisothermal DSC thermograms of MCBP(BPA-ddm)s at various heating rates under a N_2 atmosphere.

Table 2. Curing Process and Kinetic Parameters of MCBP(BPA-ddm)s

Residence time (min)	T_i[a] (°C)	T_p[a] (°C)	ΔH[a] (J g^{-1})	E_a[b] (kJ mol^{-1})	n[c]
5	214	244	214	110	0.93
10	217	246	58	82	0.90
15	216	249	87	118	0.93

[a]Calculated from the thermogram of MCBP(BPA-ddm)s at a heating rate of 10 °C min^{-1}. [b]Calculated by the Kissinger method. [c]Calculated by the Crane method.

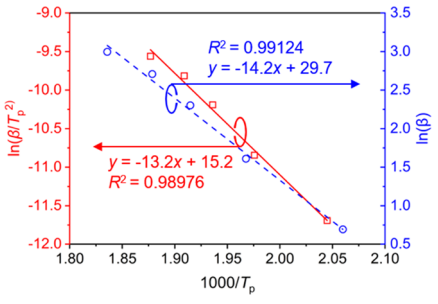

Figure 8. Kissinger plot of $\ln(\beta/T_p^2)$ and the Crane plot of $\ln\beta$ vs $1000/T_p$ for MCBP(BPA-ddm)-5.

mol^{-1}, respectively. Given that accurate E_a is obtained by the Kissinger method only in the case of a "first-order" process, the values of MCBP(BPA-ddm)s' polymerization identify the validity of the activation energy of the curing reaction. Because of the high ring-closed ratio of MCBP(BPA-ddm)s (>93%), it seems that the effects of molecular weight on the curing reaction can be negligible. But the content of the phenolic groups in the molecular matrix is the vital factor; thus, the E_a value of MCBP(BPA-ddm)-10 (82 kJ mol^{-1}) is lower than those of the other two samples due to its highest ring-opened ratio.

In short, similar thermal curing behavior is detected in all MCBP(BPA-ddm)s' systems, following the first-order curing kinetics regardless of the molecular weight. The higher the ring-opened ratio, the lower the activation energy.

4. CONCLUSIONS

A continuous-flow reactor was fabricated to synthesize the main-chain benzoxazine polymers MCBP(BPA-ddm)s in this work. The residence time for preparing MCBP(BPA-ddm)s with high M_w above 1.0×10^4 g mol^{-1} can be reduced to 5 min, suggesting the considerable time efficiency for benzoxazine synthesis by continuous flow, which also provides a good method to adjust the MCBP(BPA-ddm)s' polydispersity (2.8–3.3) by controlling the reactor's operation process. Furthermore, the high purity with >93% ring-closed ratio of MCBP(BPA-ddm)s was also confirmed using FTIR and NMR spectroscopies. The thermal curing reaction and kinetics of MCBP(BPA-ddm)s were investigated using *in situ* FTIR spectroscopy and DSC, proving their typical thermally driven self-catalyzed ring-opening polymerization profile. The apparent activation energy (E_a) and the curing reaction order (n) can be calculated using the Kissinger and Crane methods. A similar thermal curing behavior is detected by nonisothermal DSC in all MCBP(BPA-ddm)s' systems, following the first-order curing kinetics regardless of the molecular weight, which may play a secondary role in the curing process compared with the ring-opened ratio of MCBP(BPA-ddm)s. MCBP(BPA-ddm)-10 with a high ring-opened ratio of 7% shows a low E_a of 82, ~20 kJ mol^{-1} lower than those of the other two MCBP(BPA-ddm)s. Therefore, this work offers a new method for MCBP synthesis with high molecular weight and

https://doi.org/10.1021/acs.iecr.1c04771
Ind. Eng. Chem. Res. 2022, 61, 2947–2954

controllable polydispersity. Future work will focus on studying the structure−performance relationship of MCBPs and extending their high-performance applications.

■ ASSOCIATED CONTENT

Supporting Information

The Supporting Information is available free of charge at https://pubs.acs.org/doi/10.1021/acs.iecr.1c04771.

In situ FTIR spectra and the Kissinger plot of $\ln(\beta/T_p^2)$ and the Crane plot of $\ln\beta$ vs $1000/T_p$ for MCBP(BPA-ddm)-10 and MCBP(BPA-ddm)-15 (PDF)

■ AUTHOR INFORMATION

Corresponding Authors

Changlu Zhou − *Shanghai Key Laboratory of Multiphase Materials Chemical Engineering, East China University of Science and Technology, Shanghai 200237, China;* orcid.org/0000-0003-2471-2312; Email: changluzhou@ecust.edu.cn

Zhong Xin − *State Key Laboratory of Chemistry Engineering, School of Chemical Engineering, East China University of Science and Technology, Shanghai 200237, China;* orcid.org/0000-0002-6542-2699; Email: xzh@ecust.edu.cn

Authors

Zhou Zhou − *Shanghai Key Laboratory of Multiphase Materials Chemical Engineering, East China University of Science and Technology, Shanghai 200237, China*

Qian Si − *Shanghai Key Laboratory of Multiphase Materials Chemical Engineering, East China University of Science and Technology, Shanghai 200237, China*

Li Wan − *Shanghai Key Laboratory of Multiphase Materials Chemical Engineering, East China University of Science and Technology, Shanghai 200237, China*

Shiao-Wei Kuo − *Department of Materials and Optoelectronic Science, National Sun Yat-Sen University, Kaohsiung 804, Taiwan*

Complete contact information is available at: https://pubs.acs.org/10.1021/acs.iecr.1c04771

Funding

The authors acknowledge the Shanghai Pujiang Program (2020PJD015), the National Natural Science Foundation of China (21978086), Shanghai Municipal Science and Technology Commission (21520761100), the Open Project of State Key Laboratory of Chemical Engineering (SKL-ChE-21C07), and the Fundamental Research Funds for the Central Universities, Science and Technology Commission of Shanghai Municipality (20DZ2254500).

Notes

The authors declare no competing financial interest.

■ REFERENCES

(1) Lyu, Y.; Ishida, H. Natural-sourced benzoxazine resins, homopolymers, blends and composites: A review of their synthesis, manufacturing and applications. *Prog. Polym. Sci.* **2019**, *99*, No. 101168.

(2) Yagci, Y.; Kiskan, B.; Ghosh, N. N. Recent advancement on polybenzoxazine—A newly developed high performance thermoset. *J. Polym. Sci., Part A: Polym. Chem.* **2009**, *47*, 5565−5576.

(3) Mohamed, M. G.; Kuo, S. W. Functional Silica and Carbon Nanocomposites Based on Polybenzoxazines. *Macromol. Chem. Phys.* **2019**, *220*, No. 1800306.

(4) Higginson, C. J.; Malollari, K. G.; Xu, Y.; Kelleghan, A. V.; Ricapito, N. G.; Messersmith, P. B. Bioinspired Design Provides High-Strength Benzoxazine Structural Adhesives. *Angew. Chem.* **2019**, *131*, 12399−12407.

(5) Zhang, K.; Han, M.; Liu, Y.; Froimowicz, P. Design and synthesis of bio-based high-performance trioxazine benzoxazine resin via natural renewable resources. *ACS Sustainable Chem. Eng.* **2019**, *7*, 9399−9407.

(6) Zhang, K.; Liu, Y.; Han, M.; Froimowicz, P. Smart and sustainable design of latent catalyst-containing benzoxazine-bio-resins and application studies. *Green Chem.* **2020**, *22*, 1209−1219.

(7) Salum, M. L.; Iguchi, D.; Arza, C. R.; Han, L.; Ishida, H.; Froimowicz, P. Making Benzoxazines Greener: Design, Synthesis, and Polymerization of a Biobased Benzoxazine Fulfilling Two Principles of Green Chemistry. *ACS Sustainable Chem. Eng.* **2018**, *6*, 13096−13106.

(8) Chen, J.; Zeng, M.; Feng, Z.; Pang, T.; Huang, Y.; Xu, Q. Design and Preparation of Benzoxazine Resin with High-Frequency Low Dielectric Constants and Ultralow Dielectric Losses. *ACS Appl. Polym. Mater.* **2019**, *1*, 625−630.

(9) Lin, C. H.; Chang, S. L.; Shen, T. Y.; Shih, Y. S.; Lin, H. T.; Wang, C. F. Flexible polybenzoxazine thermosets with high glass transition temperatures and low surface free energies. *Polym. Chem.* **2012**, *3*, 935−945.

(10) Zeng, M.; Chen, J.; Xu, Q.; Huang, Y.; Feng, Z.; Gu, Y. A facile method for the preparation of aliphatic main-chain benzoxazine copolymers with high-frequency low dielectric constants. *Polym. Chem.* **2018**, *9*, 2913−2925.

(11) Kaya, G.; Kiskan, B.; Yagci, Y. Coumarines as masked phenols for amide functional benzoxazines. *Polym. Chem.* **2019**, *10*, 1268−1275.

(12) Liu, J.; Wuliu, Y.; Dai, J.; Hu, J.; Liu, X. Synthesis and properties of the bio-based isomeric benzoxazine resins: Revealing the effect of the neglected short alkyl substituents. *Eur. Polym. J.* **2021**, *157*, No. 110671.

(13) Allen, D. J.; Ishida, H. Effect of phenol substitution on the network structure and properties of linear aliphatic diamine-based benzoxazines. *Polymer* **2009**, *50*, 613−626.

(14) Alhassan, S.; Schiraldi, D.; Qutubuddin, S.; Agag, T.; Ishida, H. Various Approaches for Main-chain Type Benzoxazine Polymers. In *Handbook of Benzoxazine Resins*; Elsevier, 2011; Vol. *32*, pp 309−318.

(15) Takeichi, T.; Kano, T.; Agag, T. Synthesis and thermal cure of high molecular weight polybenzoxazine precursors and the properties of the thermosets. *Polymer* **2005**, *46*, 12172−12180.

(16) Chernykh, A.; Liu, J.; Ishida, H. Synthesis and properties of a new crosslinkable polymer containing benzoxazine moiety in the main chain. *Polymer* **2006**, *47*, 7664−7669.

(17) Velez-Herrera, P.; Doyama, K.; Abe, H.; Ishida, H. Synthesis and Characterization of Highly Fluorinated Polymer with the Benzoxazine Moiety in the Main Chain. *Macromolecules* **2008**, *41*, 9704−9714.

(18) Wang, L.; Zheng, S. Morphology and thermomechanical properties of main-chain polybenzoxazine-block-polydimethylsiloxane multiblock copolymers. *Polymer* **2010**, *51*, 1124−1132.

(19) Takeichi, T.; Kano, T.; Agag, T.; Kawauchi, T.; Furukawa, N. Preparation of high molecular weight polybenzoxazine prepolymers containing siloxane unites and properties of their thermosets. *J. Polym. Sci., Part A: Polym. Chem.* **2010**, *48*, 5945−5952.

(20) Agag, T.; Geiger, S.; Alhassan, S. M.; Qutubuddin, S.; Ishida, H. Low-Viscosity Polyether-Based Main-Chain Benzoxazine Polymers: Precursors for Flexible Thermosetting Polymers. *Macromolecules* **2010**, *43*, 7122−7127.

(21) Agag, T.; Takeichi, T. High-molecular-weight AB-type benzoxazines as new precursors for high-performance thermosets. *J. Polym. Sci., Part A: Polym. Chem.* **2007**, *45*, 1878−1888.

(22) Kobayashi, T.; Muraoka, M.; Goto, M.; Minami, M.; Sogawa, H.; Sanda, F. Main-chain type benzoxazine polymers consisting of

polypropylene glycol and phenyleneethynylene units: spacer effect on curing behavior and thermomechanical properties. *Polym. J.* **2022**, *54*, 133−141.
(23) Nagai, A.; Kamei, Y.; Wang, X.-S.; Omura, M.; Sudo, A.; Nishida, H.; Kawamoto, E.; Endo, T. Synthesis and crosslinking behavior of a novel linear polymer bearing 1,2,3-triazol and benzoxazine groups in the main chain by a step-growth click-coupling reaction. *J. Polym. Sci., Part A: Polym. Chem.* **2008**, *46*, 2316−2325.
(24) Liu, Y.-L.; Chou, C.-I. High performance benzoxazine monomers and polymers containing furan groups. *J. Polym. Sci., Part A: Polym. Chem.* **2005**, *43*, 5267−5282.
(25) Agag, T. Preparation and properties of some thermosets derived from allyl-functional naphthoxazines. *J. Appl. Polym. Sci.* **2006**, *100*, 3769−3777.
(26) Chernykh, A.; Agag, T.; Ishida, H. Effect of Polymerizing Diacetylene Groups on the Lowering of Polymerization Temperature of Benzoxazine Groups in the Highly Thermally Stable, Main-Chain-Type Polybenzoxazines. *Macromolecules* **2009**, *42*, 5121−5127.
(27) Gutmann, B.; Cantillo, D.; Kappe, C. O. Continuous-Flow Technology—A Tool for the Safe Manufacturing of Active Pharmaceutical Ingredients. *Angew. Chem., Int. Ed.* **2015**, *54*, 6688−6728.
(28) Baumann, M.; Moody, T. S.; Smyth, M.; Wharry, S. A Perspective on Continuous Flow Chemistry in the Pharmaceutical Industry. *Org. Process Res. Dev.* **2020**, *24*, 1802−1813.
(29) Akwi, F. M.; Watts, P. Continuous flow chemistry: where are we now? Recent applications, challenges and limitations. *Chem. Commun.* **2018**, *54*, 13894−13928.
(30) Pellegatti, L.; Sedelmeier, J. Synthesis of Vildagliptin Utilizing Continuous Flow and Batch Technologies. *Org. Process Res. Dev.* **2015**, *19*, 551−554.
(31) Cole, K. P.; Johnson, M. D. Continuous flow technology vs. the batch-by-batch approach to produce pharmaceutical compounds. *Expert Rev. Clin. Pharmacol.* **2018**, *11*, 5−13.
(32) Ishida, H. Process for preparation of benzoxazine compounds in solventless systems. Google Patents, 1996.
(33) Frazee, A. S. *Preparation of Benzoxazine Monomers and Prepolymers from Continuous Reactor: Effects of Molecular Architecture on Properties*; The University of Southern Mississippi, 2017.
(34) Liu, Y.; Yin, R.; Yu, X.; Zhang, K. Modification of Solventless-Synthesized Benzoxazine Resin by Phthalonitrile Group: An Effective Approach for Enhancing Thermal Stability of Polybenzoxazines. *Macromol. Chem. Phys.* **2019**, *220*, No. 1800291.
(35) Mohamed, M. G.; Chen, T.-C.; Kuo, S.-W. Solid-State Chemical Transformations to Enhance Gas Capture in Benzoxazine-Linked Conjugated Microporous Polymers. *Macromolecules* **2021**, *54*, 5866−5877.
(36) Han, L.; Iguchi, D.; Gil, P.; Heyl, T. R.; Sedwick, V. M.; Arza, C. R.; Ohashi, S.; Lacks, D. J.; Ishida, H. Oxazine Ring-Related Vibrational Modes of Benzoxazine Monomers Using Fully Aromatically Substituted, Deuterated, 15N Isotope Exchanged, and Oxazine-Ring-Substituted Compounds and Theoretical Calculations. *J. Phys. Chem. A* **2017**, *121*, 6269−6282.
(37) Zhou, C.; Fu, M.; Xie, H.; Gong, Y.; Chen, J.; Liu, J.; Xin, Z. Polybenzoxazine/Epoxy Composite Coatings: Effect of Crosslinking on Corrosion Resistance. *Ind. Eng. Chem. Res.* **2021**, *60*, 1675−1683.
(38) Kaya, Ş. *Synthesis and Characterization of a Polybenzoxazine from a Difunctional Amine and a Trifunctional Phenol*; Middle East Technical University, 2009.
(39) Deliballi, Z.; Kiskan, B.; Yagci, Y. Main-chain benzoxazine precursor block copolymers. *Polym. Chem.* **2018**, *9*, 178−183.
(40) Kaya, G.; Kiskan, B.; Yagci, Y. Phenolic Naphthoxazines as Curing Promoters for Benzoxazines. *Macromolecules* **2018**, *51*, 1688−1695.
(41) Zhang, K.; Tan, X.; Wang, Y.; Ishida, H. Unique self-catalyzed cationic ring-opening polymerization of a high performance deoxybenzoin-based 1,3-benzoxazine monomer. *Polymer* **2019**, *168*, 8−15.
(42) Zhang, S.; Yang, P.; Bai, Y.; Zhou, T.; Zhu, R.; Gu, Y. Polybenzoxazines: Thermal Responsiveness of Hydrogen Bonds and Application as Latent Curing Agents for Thermosetting Resins. *ACS Omega* **2017**, *2*, 1529−1534.
(43) Zhai, Q.; Wu, X.; Zhao, S.; Zhou, C. Curing Kinetics Study by FTIR Spectroscopy and Properties Analysis of Methyl Silicone Resin Membrane. *Silicon* **2020**, *12*, 2761−2768.
(44) Rimdusit, S.; Ishida, H. In *Kinetic Studies of Curing Process and Gelation of High Performance Thermosets based on Ternary Systems of Benzoxazine, Epoxy and Phenolic Resins*, 46th International SAMPE Symposium and Exhibition, 2001; pp 1466−1480.
(45) Xu, Q.; Zeng, M.; Chen, J.; Zeng, S.; Huang, Y.; Feng, Z.; Xu, Q.; Yan, C.; Gu, Y. Synthesis, polymerization kinetics, and high-frequency dielectric properties of novel main-chain benzoxazine copolymers. *React. Funct. Polym.* **2018**, *122*, 158−166.
(46) Zhou, J.; Zhao, C.; Liu, L.; Ding, J.; Li, Y. Catalytic effect of sulfonated poly (styrene-divinylbenzene) microspheres on the thermal curing behavior of benzoxazine. *Thermochim. Acta* **2018**, *661*, 106−115.
(47) Huang, Y.; Zeng, M.; Ren, J.; Wang, J.; Fan, L.; Xu, Q. Preparation and swelling properties of graphene oxide/poly(acrylic acid-co-acrylamide) super-absorbent hydrogel nanocomposites. *Colloids Surf., A* **2012**, *401*, 97−106.
(48) Mohamed, M. G.; Kuo, S.-W. Crown Ether-Functionalized Polybenzoxazine for Metal Ion Adsorption. *Macromolecules* **2020**, *53*, 2420−2429.

https://doi.org/10.1021/acs.iecr.1c04771
Ind. Eng. Chem. Res. 2022, 61, 2947−2954